AN IMPROVED CLASSIFICATION SCHEME FOR STANDOFF DETECTION OF EXPLOSIVES VIA RAMAN SPECTROSCOPY

Naveed R. Butt ⋆, *Mikael Nilsson*†, *Andreas Jakobsson*⋆, *Anna Pettersson*‡, *Sara Wallin*‡, *and Henric Oestmark*‡

ABSTRACT

Raman spectroscopy is a laser-based vibrational technique that can provide spectral signatures unique to a multitude of compounds. The technique is gaining widespread interest as a method for detecting hidden explosives due to its sensitivity and ease of use. In this work, we present a computationally efficient classification scheme for accurate standoff identification of several common explosives using visible-range Raman spectroscopy. Using real measurements, we evaluate and modify a recent correlation-based approach to classify Raman spectra from various both harmful and commonplace substances. The results show that the proposed approach can, at a distance of 30 meters, or more, successfully classify measured Raman spectra from several explosive substances, including Nitromethane, TNT, DNT, Hydrogen Peroxide, TATP and Ammonium Nitrate.

1. INTRODUCTION

Raman spectroscopy is a powerful non-contact technique that uses a laser to probe the vibrational energy levels of molecules in a substance [1]. The vibration information provided by a Raman spectrum is very specific for the chemical composition of the molecules. The spectrum can therefore provide unique signature for identification of vapor traces from various materials [2]. Recently, Raman spectroscopy has been receiving increased attention as a stand-off explosive detection technique [3,4]. Some of the important security applications being investigated include detection of improvised explosive devices (IEDs) from a safe distance in hostile environments, and scanning of vehicles and personnel at airports, international borders and in subways to detect explosive residue (see, e.g., [5] and references therein).

In general, a Raman spectrum consists of peaks that correspond to the characteristic vibrational frequencies of a material. As a result, one may, for the substances of interest, collect Raman spectra with very high signal-to-noise ratio (SNR) under laboratory conditions. These 'reference' spectra can then be stored in a database as a signature for the particular substance. A common Raman-based detection system uses laser to energize molecules in or on an object and collects the resulting Raman scattered light with a telescope. The spectrum produced by the collected light can then be analyzed and classified using the reference database. The correct identification and subsequent classification of a measured spectrum is crucial to the successful application of Raman spectroscopy to explosive detection. An important limiting factor in the use of visible-range Raman spectroscopy is the presence of strong background florescence originating from the substance of interest or its surroundings. Some of the common approaches to overcoming this limitation are, for instance, the use of near-infrared or ultra-violet excitation [3, 5], or the removal of the background florescence using computationally expensive techniques such as neural networks or fuzzy models (see, e.g., [6] and [7]). In this work, we present a computationally efficient classification scheme for accurate standoff identification of several common explosives using visible-range excitation. In the first stage of the proposed technique, we process a measured Raman spectrum through a series of simplistic median filters to efficiently model and remove the cosmic noise and the background florescence. The processed spectrum is then matched against the reference database using the recently developed correlation-bound approach, where the upper bound of the correlation between the measured spectrum and each reference spectrum is used as a detection index [8]. The detection index is normalized to be in the range [0 1], with 1 representing a complete match. The results show that the used approach can, at a distance of 30 meters, or more, successfully classify measured Raman spectra from several explosive substances, including Nitromethane, TNT, DNT, Hydrogen Peroxide, TATP and Ammonium Nitrate.

Notation: $(\cdot)^T$ is used to represent the transpose. Vectors are denoted with bold letters, $\mathbf{y}$, while scalars are in light-face, y.

2. EXPERIMENTAL SETUP

The characterization of explosives using Raman spectroscopy was suggested by Urbanski in 1964 [9]. The technique has recently received increased attention due to improvements in instrumentation and signal processing, which make it a strong candidate for detection of trace explosives at a safe distance. As noted in the introduction, it is possible to collect Raman spectra with high SNR for substances of interest. These spectra provide unique signatures of different explosive substances, which can be used to detect the presence of a threat.

⋆N. R. Butt and A. Jakobsson are with the Center for Mathematical Sciences, Lund University, SE-22100 Lund, Sweden (email:naveed@maths.lth.se; andreas.jakobsson@ieee.org).

†Mikael Nilsson is with the Department of Electrical Engineering, Blekinge Institute of Technology, Ronneby, Sweden (email:mikael.nilsson@bth.se).

‡Anna Pettersson, Sara Wallin and Henric Oestmark are with the Swedish Defence Research Agency, 147 25 Tumba, Sweden.

 ISSN 2076-1465

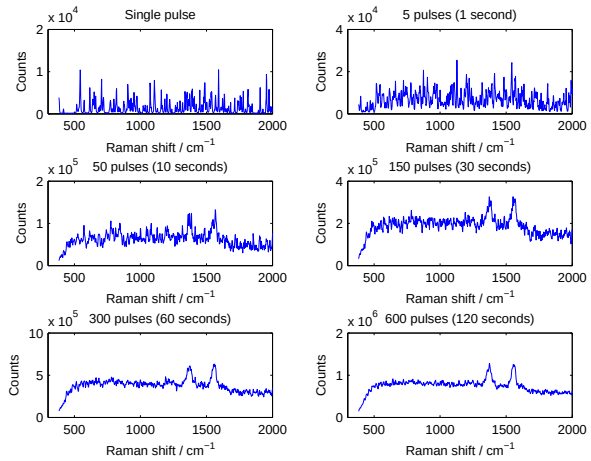

Figure 1: Raman spectra from 0.25mg TNT, measured at a distance of 30 meters. The figure shows the single-pulse measurements as well as results of coherently adding several measurements to increase the SNR.

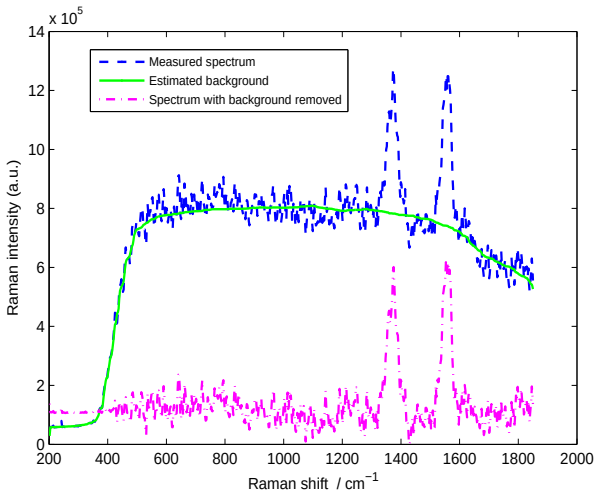

Figure 2: Removing the effect of background florescence in a TNT spectrum. In the figure, the dashed spectrum corresponds to $\mathbf{y}$, the solid line to $\breve{\mathbf{y}}$, and the dash-dotted spectrum to $\tilde{\mathbf{z}}$.

Such 'reference' spectra from explosive substances of interest are collected under laboratory conditions and stored in a database. The reference spectra are then used to identify Raman spectra collected from targets at a safe distance. In this work, we investigate the classification of Raman spectra from several common explosives, including TNT, TATP and Ammonium Nitrate. However, we note that the developed framework is quite general and can be used for classification of other explosive substances as well. For the purpose of this study, we collected real Raman spectra at Gridsjön, Sweden, in collaboration with personnel from Portendo Inc. A pulsed Nd:YAG laser (NL-303HT from Ekspla) was aimed at the target at a range of 30 m by a YAG-coated mirror. The laser was operated at 5 Hz with 4 ns long pulses and a wavelength of 532 nm. The Raman scattered light was collected at an oblique angle from the incident laser beam and through a Newtonian telescope. After the telescope, two fused silica lenses were used to focus the light into an optical fiber and a Raman long pass filter from Semrock was placed between the lenses to block the laser line. The slit end of the fiber was connected to an f-number matcher (SR-ASM-0018) mounted on the Andor SR-303i-A spectrometer. On the spectrometer, a gated ICCD camera (DH-740I-18F-03 from Andor) was mounted. The gate time of the ICCD was set to 10 ns. A more detailed description of the experimental setup is available in [10]. Typical spectra collected from 0.25mg of TNT using this approach are shown in Figure 1. The figure shows the single-pulse measurements as well as results of coherently adding several single-pulse measurements to increase the SNR. As is well known, Raman spectroscopy suffers from background florescence [2, 6]. The effect of background florescence can be seen more clearly in the multi-pulse measurements as a general wave-like lifting of the baseline. The removal of the background effect will be discussed in detail in the next section.

3. PREPROCESSING AND CLASSIFICATION

Given two length N vectors, $\mathbf{r}$ and $\mathbf{y}$, containing the amplitudes of the reference and measured Raman spectra, respectively, and with $\mathbf{r}$ centralized and normalized so that $\sum_i r_i/N = 0$, $\sum_i r_i^2 = 1$, the square of the upper correlation bound between the two vectors may be evaluated as [8]

$$\rho^2 = \mathrm{corr}^2_{max}(\mathbf{r}, \mathbf{y}) = \mathbf{r}^T \hat{\mathbf{y}} (\hat{\mathbf{y}}^T \hat{\mathbf{y}})^{-1} \hat{\mathbf{y}}^T \mathbf{r}, \qquad (1)$$

where

$$\hat{\mathbf{y}} = \mathbf{y} - \mathbf{1} \frac{\sum_i y_i}{N}, \qquad (2)$$

with $\mathbf{1}$ representing a column vector of 1's. The correlation bound assigns a score to the degree of similarity between a reference and a measured spectrum. As is clear from (1), the maximum score is unity and is obtained only for a perfect match, i.e., for $\mathbf{y} = \mathbf{r}$. A measured spectrum can thus be compared against a database of reference spectra using the correlation bound, and the resulting scores can be used for possible classification of the measured spectrum. As is shown in [8], the correlation bound approach provides better overall performance and robustness as compared to the other more commonly used techniques in Raman spectroscopy, including generalized likelihood ration test (GLRT) and independent component analysis (ICA) [11]. However, the performance of the correlation bound approach is strongly affected by the background florescence as well as by cosmic noise commonly present in the measured spectra. The cosmic noise typically introduces a sum of impulsive spikes at random wavelengths. Approaches to reduce this kind of noise can be found in literature [7,12]. Here, we adopt the median filter [12] due to its simplicity and rapid calculation compared to other techniques such as Fuzzy methods [7]. Here, a noise-spike is defined as a 'peak' with the Full Width at Half Maximum

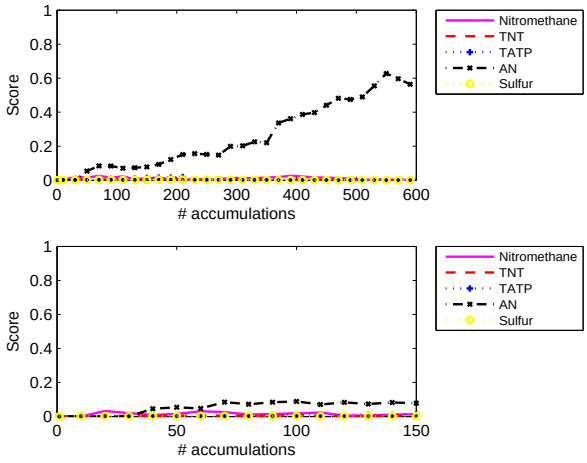

Figure 3: Top: correlation bound scores for spectrum from 0.5mg Ammonium Nitrate versus accumulations. Bottom: magnified view of the first 150 accumulations.

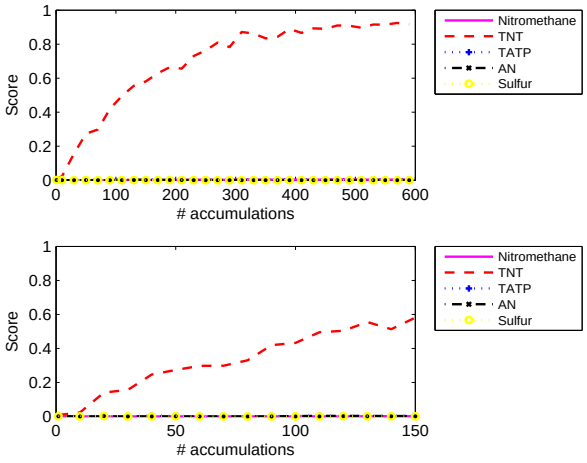

Figure 4: Top: correlation bound scores for spectrum from 0.25mg TNT against increasing accumulations. Bottom: magnified view of the first 150 accumulations.

(FWHM) smaller than the reasonable minimum a Raman peak could have. The new signal containing none, or less, cosmic noise can be found as

$$\tilde{\mathbf{y}} : \tilde{y}_i = \text{med}\{y_{i-(\tilde{n}-1)/2}, \ldots, y_{i+(\tilde{n}-1)/2}\}, \tag{3}$$

where the filter length, $\tilde{n}$, is chosen to keep the smallest possible Raman peak and to remove impulses in the spectrum. After the cosmic noise is filtered out, we proceed to process the measurement vector to remove the background florescence without significantly affecting the characteristic peaks. To achieve this, the trend added by the background florescence is first estimated using another median filter as

$$\breve{\mathbf{y}} : \breve{y}_i = \text{med}\{\tilde{y}_{i-(n-1)/2}, \ldots, \tilde{y}_{i+(n-1)/2}\}, \tag{4}$$

where n is chosen much larger than $\tilde{n}$ to get a smooth estimate of the background florescence. The measured spectrum is then detrended by subtracting $\breve{\mathbf{y}}$ from $\tilde{\mathbf{y}}$, forming the measured preprocessed vector $\mathbf{z}$, i.e.,

$$\mathbf{z} \triangleq \tilde{\mathbf{y}} - \breve{\mathbf{y}}. \tag{5}$$

Since, by definition, the Raman amplitudes are always positive, the detrended spectrum, $\mathbf{z}$, is shifted up to remove any negative values due to the subtraction in (5), i.e.,

$$\tilde{\mathbf{z}} = \mathbf{z} - \min\big(0, \min(\mathbf{z})\big). \tag{6}$$

Figure 2 shows the removal of background florescence effect from a typical spectrum of TNT using the proposed approach in (4)-(6). Finally, to reduce the effect of the noise floor on the correlation bound, we null all values below a certain threshold. This is achieved by forming a 'cleaner' vector $\mathbf{x}$ as

$$\mathbf{x} : x_i = \begin{cases} 0 & \text{for } \tilde{z}_i \leq \eta \cdot \max(\tilde{\mathbf{z}}) \\ \tilde{z}_i & \text{otherwise.} \end{cases} \tag{7}$$

where η is a small fraction, chosen to reflect the expected level of the noise floor. We may now rewrite the correlation bound using the preprocessed measurement vector, $\mathbf{x}$, as

$$\tilde{\rho}^2 = \text{corr}^2_{max}(\mathbf{r}, \mathbf{x}) = \mathbf{r}^T \hat{\mathbf{x}} (\hat{\mathbf{x}}^T \hat{\mathbf{x}})^{-1} \hat{\mathbf{x}}^T \mathbf{r}, \tag{8}$$

where $\hat{\mathbf{x}}$ is defined similar to $\hat{\mathbf{y}}$.

4. RESULTS AND DISCUSSIONS

To demonstrate the effectiveness of the proposed approach in standoff detection of explosives, the algorithm was tested on real Raman spectra collected, at a distance of 30 meters, from different quantities of the commonly used explosives Nitromethane, TNT, DNT, TATP, Hydrogen Peroxide, Ammonium Nitrate and sulfur, as well as several others commonplace interfering materials including CCD noise, Aluminium plate, red colored car door, petrol, diesel, methanol, engine oil, wax, empty glass bottle, glass bottle with tap water, earth and sand, leaves, tree bark and dandelions. The experimental setup has been detailed in Section 2. High SNR reference spectra for the explosive class were formed by coherently accumulating 600 single-pulse measurements. Both the reference spectra and the measured spectra were preprocessed according to (3)-(7). To get a smooth estimate of the background florescence, a long median filter with $n = 300$ samples, was applied. After close inspection of the measured spectra under experimental conditions, the noise threshold level, η, in (7) was set to 0.2, while $\tilde{n}$ was chosen as 5 samples. Finally, the measured spectra were processed to remove the commonly appearing Oxygen peak at 1550cm^{-1}.

The proposed algorithm was first tested for its ability to distinguish between different explosives based on the similarity scores it assigns to each measured spectrum against reference spectra of Nitromethane, TNT, TATP, Ammonium Nitrate and Sulfur, according to the correlation bound formulation (8). Typical classifier scores for spectra from Ammonium Nitrate and TNT are shown

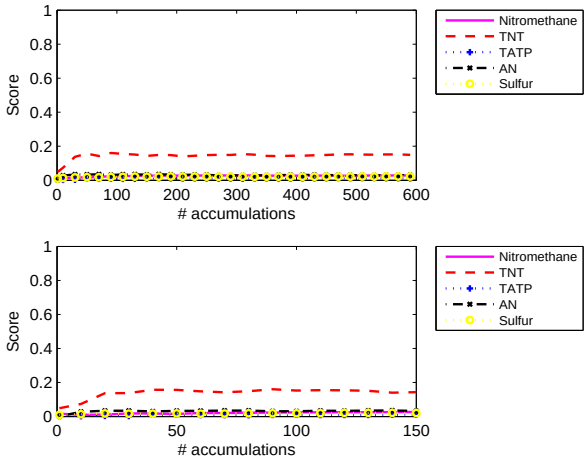

Figure 5: Top: correlation bound scores for spectrum from 0.25mg TNT, without applying the proposed preprocessing. Bottom: magnified view of the first 150 accumulations.

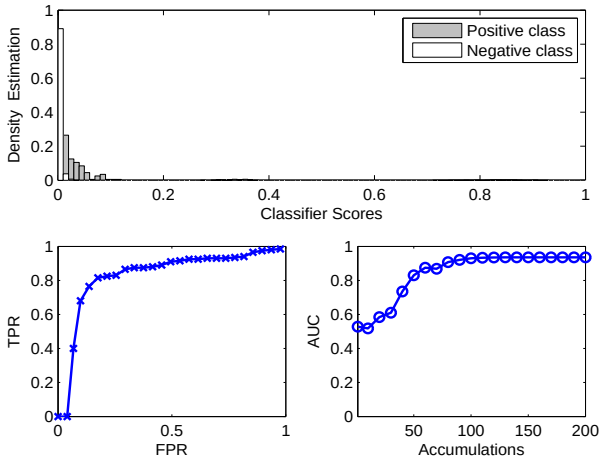

Figure 6: Analysis of detection performance for 0.5mg Ammonium Nitrate. Top: classifier scores for 50 accumulations. Bottom left: ROC curve for 50 accumulations. Bottom right: AUC plot versus accumulations.

in figures 3 and 4, respectively. The scores are plotted against increasing numbers of summed scans, called accumulations, for each measurement, as Raman measurements can be added coherently to improve the SNR. As is clear from these figures, the proposed scheme assigns the highest scores to the correct chemical in each case. Despite the relatively small quantity of the explosive being tested, the explosive was correctly identified as TNT. We note that similar results were obtained for the remaining explosives under study. To illustrate the benefits of the proposed preprocessing stages discussed in Section 3, Figure 5 shows the correlation bound scores for the data in Figure 4 when this preprocessing has not been applied. As is clear from the comparison between Figures 4 and 5, the suggested modifications significantly improve the detection performance of the method.

In critical applications such as detection of IEDs, it is important to detect the presence of explosives with a high true positive rate (TPR) and a low false positive rate (FPR). For this purpose, the performance of the proposed scheme was analyzed with the help of receiver operation characteristic (ROC) curves [13] and the area under the ROC (AUC) curves. The ROC curves plot TPR against FPR, while the AUC shows the area under the ROC curves; which is the probability that the classifier will assign higher score to a randomly chosen member of the positive class than a randomly chosen member of the negative class. In this study, a ROC curve for a particular explosive is evaluated using up to 200 measurements of that explosive as the positive class and 200 measurements of each of the other explosives and interferers as the negative class. Figures 6 and 7 show typical results for Ammonium Nitrate and TNT, respectively. In each of these figures, the top plot shows the histogram of the classifier scores for 50 accumulations, the bottom left plot shows the ROC curve at 50 accumulations and the bottom right plot shows the AUC values against increasing accumulations of single-pulse measurements. Here, a ROC curve for K accumulations means that it was evaluated using data formed by adding K single-scan measurements. It is clear from the figures that the proposed classifier is capable of providing very reliable detection of these common explosives in the presence of commonplace interferers. We note that similar results were obtained for the remaining explosives under study. It is worth noting that there is a difference between detection of an explosive, and the correct classification of the actual explosive. For obvious reasons, one is often most interested in a rapid and reliable detection of an explosive, while only in a second, less time-critical, stage one wishes to actually identify the explosive uniquely. To illustrate a way to achieve this, we propose a two-stage approach for detection and identification of explosives and related compounds with heavily overlapping spectra, such as TNT and DNT. The purpose of the first stage is to first detect the presence of either of the two chemically similar compounds. Following a positive detection in the first stage, the classifier in the second stage attempts to identify the measured spectrum. Figure 7 shows the results of the detection stage where both TNT and DNT are treated as the positive class and the detection of either will trigger an alarm. Following the detection of TNT or DNT, the target spectrum is passed through another correlation-based classifier that uses only the peaks that are uncommon between TNT and DNT to form their respective masks. This results in the proper categorization of a spectrum originating from these chemically similar explosives. The scores of the second stage classifier are shown in Figure 8 for spectra from 0.25mg of TNT. As clear from the figure, the second stage classifier assigns higher scores to the correct explosive substance, i.e., TNT. The two-stage scheme thus gives a higher likelihood of correctly detecting TNT as compared to a single-stage approach.

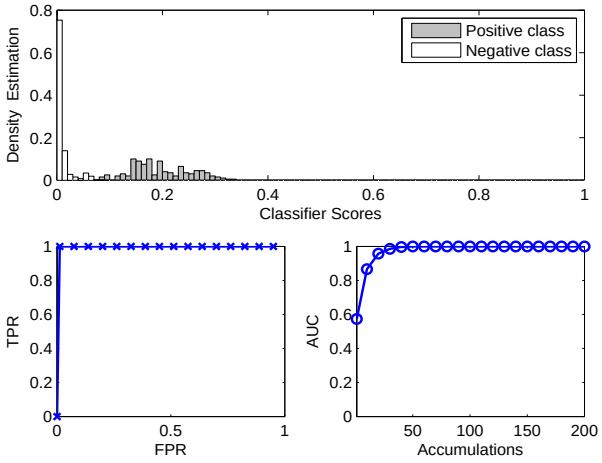

Figure 7: Analysis of detection performance for 0.25mg of TNT or DNT. Top: classifier scores for 50 accumulations. Bottom left: ROC curve for 50 accumulations. Bottom right: AUC plot versus accumulations.

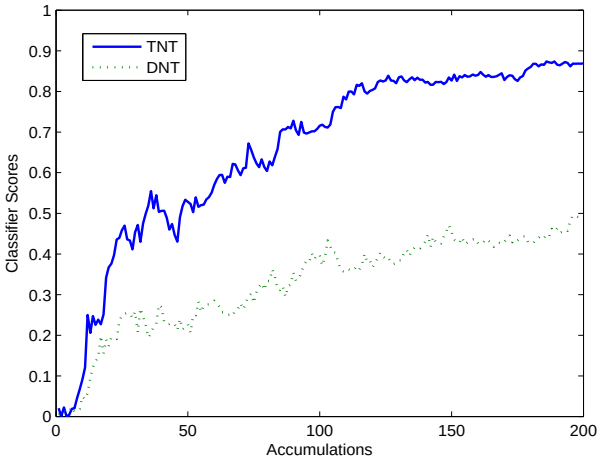

Figure 8: Second-stage classifier scores to distinguish between TNT and DNT. The measured spectra are from 0.25mg of TNT.

5. CONCLUSION

An experimental study of the application of Raman spectroscopy to stand-off detection of several common explosives is presented. Using real measurements, we evaluate and modify a recent correlation-based approach to classify Raman spectra from various both harmful and commonplace substances. The results show that the proposed approach can, at a distance of 30 meters, or more, successfully classify measured Raman spectra from several explosive substances, including Nitromethane, TNT, DNT, TATP, Hydrogen Peroxide and Ammonium Nitrate.

Acknowledgment

This work was supported in part by the Swedish Agency for Innovation Systems; the Swedish Emergency Management Agency; the Swedish Defence Material Administration; the Swedish Research Council and Carl Trygger's Foundation, Sweden.

REFERENCES

[1] D. J. Gardiner, *Practical Raman Spectroscopy*. Springer-Verlag, 1989.

[2] R. L. McCreery, *Raman Spectroscopy for chemical analysis*. John Wiley & Sons, 2000.

[3] M. Gaft and L. Nagli, "Standoff laser-based spectroscopy for explosives detection," in *Society of Photo-Optical Instrumentation Engineers (SPIE) Conference Series*, ser. Society of Photo-Optical Instrumentation Engineers (SPIE) Conference Series, vol. 6739, Oct. 2007.

[4] S. Wolf, P. J. Wrzesinski, and M. Dantus, "Standoff chemical detection using single-beam CARS," in *Conference on Lasers and Electro-Optics/International Quantum Electronics Conference*, ser. OSA Technical Digest, 2009.

[5] S. Wallin, A. Pettersson, H. Östmark, and A. Hobro, "Laser-based standoff detection of explosives: a critical review," *Anal Bioanal Chem*, vol. 395, pp. 259–274, 2009.

[6] S. Sigurdsson, J. Larsen, P. A. Philipsen, M. Gniadecka, H. C. Wulf, and L. K. Hansen, "Estimating and suppressing background in Raman spectra with an artificial neural network," in *IMM-Technical report-2003-20*, 2003.

[7] M. J. Soneira, R. Perez-Pueyo, and S. Ruiz-Moreno, "Raman spectra enhancement with a fuzzy logic approach," *Journal of Raman spectroscopy*, vol. 33, pp. 599–603, 2002.

[8] W. Wang and T. Adali, "Detection using correlation bound in a linear mixture model," *Signal Processing*, vol. 87, pp. 1118–1127, 2007.

[9] T. Urbanski, *Chemistry and technology of explosives (I)*. Pergamon, New York, 1964.

[10] A. Pettersson, I. Johansson, S. Wallin, M. Nordberg, and H. Östmark, "Near real-time standoff detection of explosives in a realistic outdoor environment at 55 m distance," *Propellants Explos. Pyrotech*, vol. 34, pp. 297–306, 2009.

[11] W. Wang and T. Adali, "Constrained ICA and its application to raman spectroscopy," in *IEEE Antennas and Propagation Scoiety Internaitonal Symposium*, vol. 4B, Washington, DC., July 2005, pp. 109–112.

[12] J. W. Tukey, "Nonlinear (nonsuperposable) methods for smoothing data," in *Conf. Rec.*, 1974 EASCON, p. 673.

[13] T. Fawcett, "ROC graphs: notes and practical considerations for researchers," in *Tech. Rep., HP Laboratories, MS 1143.*, 1501 Page Mill Road, Palo Alto CA 94304, USA., 2004.